

Harnessing dynamic metabolomics for bioprocess prediction and beyond

Wang, Guan; Haringa, Cees; Chu, Ju; Zhuang, Yingping; van Winden, Wouter; Noorman, Henk

DOI

[10.1201/9781003055211-48](https://doi.org/10.1201/9781003055211-48)

Publication date

2024

Document Version

Final published version

Published in

Handbook of Molecular Biotechnology

Citation (APA)

Wang, G., Haringa, C., Chu, J., Zhuang, Y., van Winden, W., & Noorman, H. (2024). Harnessing dynamic metabolomics for bioprocess prediction and beyond. In D. Liu (Ed.), *Handbook of Molecular Biotechnology* (pp. 460-472). CRC Press / Balkema - Taylor & Francis Group. <https://doi.org/10.1201/9781003055211-48>

Important note

To cite this publication, please use the final published version (if applicable). Please check the document version above.

Copyright

Other than for strictly personal use, it is not permitted to download, forward or distribute the text or part of it, without the consent of the author(s) and/or copyright holder(s), unless the work is under an open content license such as Creative Commons.

Takedown policy

Please contact us and provide details if you believe this document breaches copyrights. We will remove access to the work immediately and investigate your claim.

Green Open Access added to TU Delft Institutional Repository

'You share, we take care!' - Taverne project

<https://www.openaccess.nl/en/you-share-we-take-care>

Otherwise as indicated in the copyright section: the publisher is the copyright holder of this work and the author uses the Dutch legislation to make this work public.

44 Harnessing Dynamic Metabolomics for Bioprocess Prediction and Beyond

Guan Wang, Cees Haringa, Ju Chu, Yingping Zhuang, Wouter van Winden and Henk Noorman

44.1 FUNCTIONAL METABOLOMICS FOR DESCRIBING THE BIOSYNTHETIC REGULOME

Systems biology aims to gain quantitative insight into the mechanism in biological systems, which in turn provides informative cues to guide synthetic design.^{1,2} As illustrated in Figure 44.1, metabolism-centric trans-omics assays have been applied to measure spatiotemporal dynamics of the global biochemical networks that govern cellular functions.³ Alongside genomics, transcriptomics, and proteomics, metabolomics is the youngest systems biology tool that aims to identify and quantify the metabolome – the dynamic set of all small molecules (generally molecular weight <1, 500 Da) present in an organism or a biological sample in response to environmental, nutritional, or immunological stimuli. The term “metabolome” was first introduced in 1998,⁴ and nowadays, metabolomics finds increasing applications in diverse fields, from metabolic disorders to cancer, from nutrition and wellness to the design and optimization of cell factories.⁵ In addition to metabolite concentrations measured by metabolomics, a complementary approach, i.e., steady state flux balancing approach, can be used to quantify metabolite flow (i.e., metabolic flux) through biochemical networks. Moreover, for dynamic fluxomics (e.g., response to substrate pulses), metabolome dynamics in combination with dynamic metabolite mass balances, which often involve stable isotopes, are needed to determine the fluxes.⁶ Furthermore, metabolic flux analysis is often needed in combination with metabolite levels to describe cellular physiology,^{7,8} assess metabolic pathway operation^{9–11} as well as formulate metabolic model^{12,13} for systems biology and metabolic engineering.^{5,14} Previously, however, the “omics” studies other than metabolomics dominated large-scale functional analysis strategies to unravel the link between genotypes and phenotypes. Yet the downstream metabolomics has now been broadly acknowledged to show greater effects of genetic or environmental changes and thus is the most predictive of phenotype.¹⁵

In biological systems, biochemical reactions are mostly catalyzed by enzymes, and the majority of enzymes bind specific metabolites. Such interactions are highly relevant to metabolic and gene regulation.^{16,17} Protein-metabolite interactions, e.g., allosteric regulation via posttranslational protein modifications and metabolite binding, allow to rapidly coordinate metabolic flux redistribution at timescales of seconds to minutes in highly dynamic environments and/

or perturbations. Recently, it has been experimentally demonstrated that the net rates of cellular metabolic reactions are strongly driven by substrate concentrations and metabolite concentrations, which collectively have more than twice as much physiological impact as enzymes alone.¹⁸ The timescales of intracellular processes such as biochemical reactions are scale-independent (i.e., do not depend on reactor scale), whereas transport processes are not. As a consequence, the mixing time is positively correlated to the scale.¹⁹ In industrial bioprocesses, this has the most profound impact on the distribution of the limiting substrate. Highly concentrated substrate is often fed at one point in the bioreactor to minimize broth dilution. Due to mass transfer and mixing limitations, the concentration of substrate may vary over orders of magnitude in the reactor;^{20,21} in the worst-case, the substrate is in excess near the feed and depleted in the bulk,²² while the objective is to achieve a homogeneous, limiting concentration overall. A secondary consideration is that different nutrients may become limiting at different locations in the reactor. Most notably, oxygen may be limiting close to the substrate feed point, while substrate may be limiting close to the gas sparger in industrial-scale aerobic processes. Whether and how the cells react to this depends on the intracellular capacity of cells to deal with rapidly varying environments. Typically, the cells in the large-scale bioreactor are forced by the fluid flow to periodically experience high/low substrate conditions, i.e., feast/famine regime, on account of nonideal mixing and mass transfer issues.¹⁹ Often, this will result in a loss of production performance upon scaling-up, including reduced titer, yield, or productivity.²³ However, a few reports are showing that some microbial cells are seemingly insensitive to environmental perturbations at large-scale conditions,²⁴ and even in some cases, there may even be a positive effect on cellular viability,²⁵ fungal morphology²⁶ and process productivity.²⁷ Therefore, we need to assess how microbes/cells respond to rapid variations in their environment on the different ‘omics’ levels. Metabolomics plays a central role in this, as the metabolite may be directly affected by rapid variations in the extracellular environment. Subsequently, one may ask how these metabolite changes propagate into changes in the transcriptome and proteome (via, e.g., gene regulation leading to long-term phenotypic alteration or post-transcriptional regulation inducing short-term responses). In addition, due to the close relationship between metabolism and cellular phenotype, knowledge of the metabolome may serve as a basis for dynamic models of the biological

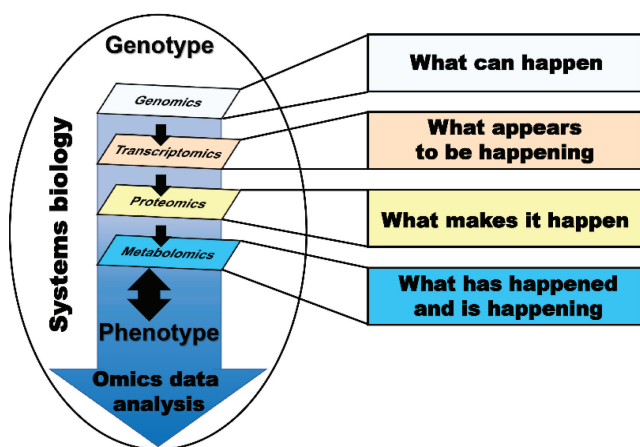


FIGURE 44.1 The “omics” cascade shows the link between genotype and phenotype. As the powerful systems biology tools, genomics, transcriptomics, proteomics, and metabolomics help determine the responses of biological systems to disease, genetic, and environmental perturbations. Being the closest to the phenotype, metabolomics provides a functional readout (metabolite level, flux change, kinetics, and thermodynamics) of cell factories.

system, capable of quantifying how the full-scale process environment impacts process performance.²⁸

To describe the whole cell physiology there are several types of cellular reaction dynamics (CRD) models describing the whole cell physiology or some aspects thereof. Genome-scale metabolic models can, in principle, provide a huge number of intracellular details via constraint-based modeling of biological networks. Although prevalently used in many applications, these models suffer from the limited mechanistic *in vivo* kinetic knowledge (e.g., lack of representation of metabolite concentrations and enzyme regulation) of each reaction.^{13,29} In contrast, the conventional black box model is capable of responding to the local environmental cues, e.g., residual glucose concentration, with minimal model complexity by neglecting all intracellular metabolic details. For instance, the saturation-type glucose uptake kinetics has been used with computational fluid dynamics (CFD) modeling to capture the glucose concentration gradient in a 30 m³ fermentation of *Saccharomyces cerevisiae*, and the coupled model predictions were favorably validated with the experimental data.²⁰ However, lacking intracellular details, this model cannot predict how this glucose concentration gradient affects the formation of (un)desired products. Nowadays, a detailed kinetic model of specific processes,³⁰ partial metabolic pathways,³¹ and large-scale kinetic models^{32–34} have become available for metabolic characterization and process prediction including intracellular dynamics. However, these more detailed metabolically kinetic models are inevitably associated with parameter estimation issues where extensive metabolic datasets are required to conduct some meaningful parameter estimation,³⁵ and also find difficulty in being integrated with the CFD model for a global assessment of industrially relevant bioprocesses. As an alternative, kinetic models

should be formulated with reduced structure yet preserved with enough dynamic features.³⁶ To achieve this, efforts have been made to replace the classical hyperbolic enzyme kinetics with more reduced and reliable models, among which six approximative kinetic formats have been recommended from the perspective of modeling efficiency.³⁷ In brief, a trade-off between modeling purpose, model complexity, simulation timeframe, and data availability for parameter identification should be taken into account when selecting the preferred CRD models for CFD coupling. In any case, it should be noted that to construct models with meaningful intracellular dynamics, metabolite quantification is required to fully exploit key intracellular mechanisms associated with cell growth and product formation.^{38,39} It is not questionable that absolute metabolite concentrations impact both metabolic reaction rates and free energies.^{40,41}

In this chapter, we demonstrate that unbiased and absolute metabolomics data can be obtained using rapid sampling, quenching, and extraction protocols in combination with the isotope dilution mass spectrometry (ID-MS) method. Based on this, metabolomics data can be applied to accelerate the learning step within the design, build, test, and learn (DBTL) cycle, guide the metabolic engineering of synthetic bioproduction pathways, and facilitate the establishment of metabolically structured models. Furthermore, a computational framework integrating the CRD model with the CFD model can be developed to evaluate the effect of environmental perturbations on the cellular metabolic behavior in industrial-scale bioreactors in high resolution.

44.2 QUANTITATIVE METABOLOMICS USING ISOTOPE DILUTION MASS SPECTROMETRY (ID-MS)

Measuring intracellular metabolites is experimentally time-consuming and tedious and is mostly constrained by technical difficulties caused by the rapid metabolite turnover rates, the need to quench metabolism, and separate them from the extracellular space with minimal metabolite leakage.⁴² In addition, quantitative metabolite profiling is further hampered by biased mass spectrometry-based analysis caused by matrix effects.⁴³ To address these issues, a complete procedure including fast sampling, immediate quenching of enzymatic activity, separation of exometabolome and endometabolome, complete metabolite extraction from the cells, and reliable high-throughput analysis method is in desperate need of obtaining quantitative snapshots of the cellular metabolome.⁴⁴

44.2.1 RAPID SAMPLING, IMMEDIATE QUENCHING AND COMPLETE EXTRACTION

The intracellular metabolite concentrations can cover a broad concentration range, roughly from 10⁻⁷ to 10⁻¹ M.⁴⁰ The turnover times of intracellular metabolite pools can be estimated based on their *in vivo* pool sizes and conversion

rates. As shown in Table 44.1, the datasets gathered from glucose-limited chemostat cultivations of *S. cerevisiae*,⁴⁵ *Penicillium chrysogenum*,^{46,47} and *Escherichia coli*⁴⁸ show that the turnover of metabolites is fast, in the order of seconds to tens of seconds, especially in the central metabolism

and energy metabolism. Rapid sampling from the bioreactor and immediate quenching of enzymatic activities is a prerequisite to obtain true snapshots of the cellular metabolism.

Over the years, several robust and reliable rapid sampling devices for metabolomics studies have been developed.^{44,49,50}

TABLE 44.1

Intracellular Metabolite Concentrations and Turnover Times in Glucose-Limited Aerobic Cultures of *Saccharomyces cerevisiae*⁴⁵, *Penicillium chrysogenum*^{46,47}, and *Escherichia coli*⁴⁸

Metabolites	Intracellular level (μmol/gDW)			Turnover time (s)		
	<i>P. chrysogenum</i>	<i>S. cerevisiae</i>	<i>E. coli</i>	<i>P. chrysogenum</i>	<i>S. cerevisiae</i>	<i>E. coli</i>
<i>Central metabolites</i>						
G6P	4.64	5.2	1.42	23.3	17	3.6
F6P	0.71	1.4	0.38	5.7	7.3	1.2
T6P	0.55		0.13	47.8		NA
M6P	1.95		0.48			NA
6PG	0.25	0.48	0.10	3.7	4.5	1.1
Mannitol-1P			0.99			NA
G3P		0.13	0.17		57	13.1
FBP	0.9	0.64	0.82	7.2	3.2	2.5
F2, 6bP	0.01		0.35			NA
2PG+3PG	0.59	2.8	1.65	2.3	6.6	2.5
PEP	0.24	2.3	1.61	0.9	5.7	2.7
Pyruvate	0.22	1.1	0.75	0.9	1.7	1.5
α-ketoglutarate	2.05		0.31	22.1		0.6
Succinate	0.23	4.0	2.65	3.3	20	8.9
Fumarate	0.65	0.85	0.22	13.0	4.1	0.7
Malate	3.33	7.3	0.94	19.0	30	2.8
<i>Amino acids</i>						
Alanine	21.7	32	1.34	269	3268	76.7
Asparagine	1.5	4.7	0.58	459	1142	81.7
Aspartate	16.3	21	2.57	717	577	35.0
Glutamate	53.0	170	74.69	658	1112	229.0
Glutamine	28.7	64	6.14	1243	2401	80.0
Glycine	2.1	2.9	1.51	244	247	31.0
Histidine	0.72	6.0	0.15	432	3141	53.8
Isoleucine	0.33	1.6	0.11	111	140	12.9
Leucine	0.73	1.0	0.36	131	125	27.1
Methionine	0.14	0.20	0.05	58.8	66	10.5
Phenylalanine	0.19	1.6	0.13	61.2	430	23.8
Proline	0.95	3.9	0.66	206	925	101.4
Serine	5.7		0.53	453		8.0
Threonine	5.9	4.0	0.47	758	220	29.3
Tryptophan	0.11	0.51	0.02	130	788	11.9
Tyrosine	0.26	1.6	0.18	145	832	44.3
Valine	2.1	10	0.51	243	490	40.9
Ornithine		4.1	0.49		502	49.1
<i>Adenine nucleotides</i>						
ATP	7.39	7.0	5.95	NA	1.4	2.0
ADP	1.03	1.3	2.31	NA	1.4	2.0
AMP	0.27	0.6	0.91	NA	3.1	9.4

Source: Reproduced from Wang et al.¹⁰² with permission of John Wiley & Sons.

These devices can be roughly divided into three categories: single-point, fast sampling device, 'stopped-flow' fast sampling device, and multi-point fast sampling device (Figure 44.2).

The types of rapid sampling devices above realize the rapid sampling of bioprocesses to some extent. Nonetheless, they have obvious shortcomings. The first type of rapid sampling device (Figure 44.2A) creates a negative pressure space by adding a vacuum pump to achieve a rapid sampling process within 1 second. However, poor applicability (the need to specify a test tube to match the test tube adapter) and poor system reliability (the negative pressure space is often prone to failure due to air leakage, resulting in sampling failure) may compromise its performance. The second type of rapid sampling device (Figure 44.2B) trades space for time and can accurately estimate the sampling time point by calculating the flow rate and distance. However, due to its fixed sampling location, the sampling process cannot be designed arbitrarily according to experimental requirements. The third type of rapid sampling device (Figure 44.2C) has a complex structure and strong system specificity, making its application to various bioreactors difficult. At the same time, because it involves a

variety of automated controls, the coordination within the system needs to be adjusted. In addition, the time point of continuous sampling is also more difficult to accurately control and to modify once determined. Moreover, the last two types of rapid sampling devices are limited by the sampling pipe diameter (dead sampling volume) and often cannot achieve rapid sampling and quenching within 1 second, and thus cannot run smoothly in case of high viscosity fermentations, e.g., filamentous fungal fermentation and polysaccharide fermentation. The off-site weighing process not only increases the time of the duration of the sampling process but also introduces an error in the sampling amount due to condensation of the cryogenic quencher. To address these issues, we have recently designed a customized rapid sampling device allowing for simple, reliable operation and broad applicability. As shown in Figure 44.2D, it achieves rapid sampling within 1 second with the aid of both bioreactor overpressure and programmed high-speed pump for discharge and rinse and introduces multiple sets of sampling pipelines with different pipe diameters, which improves the compatibility with different fermentation processes (low/high viscosity). This sampling device has been used to

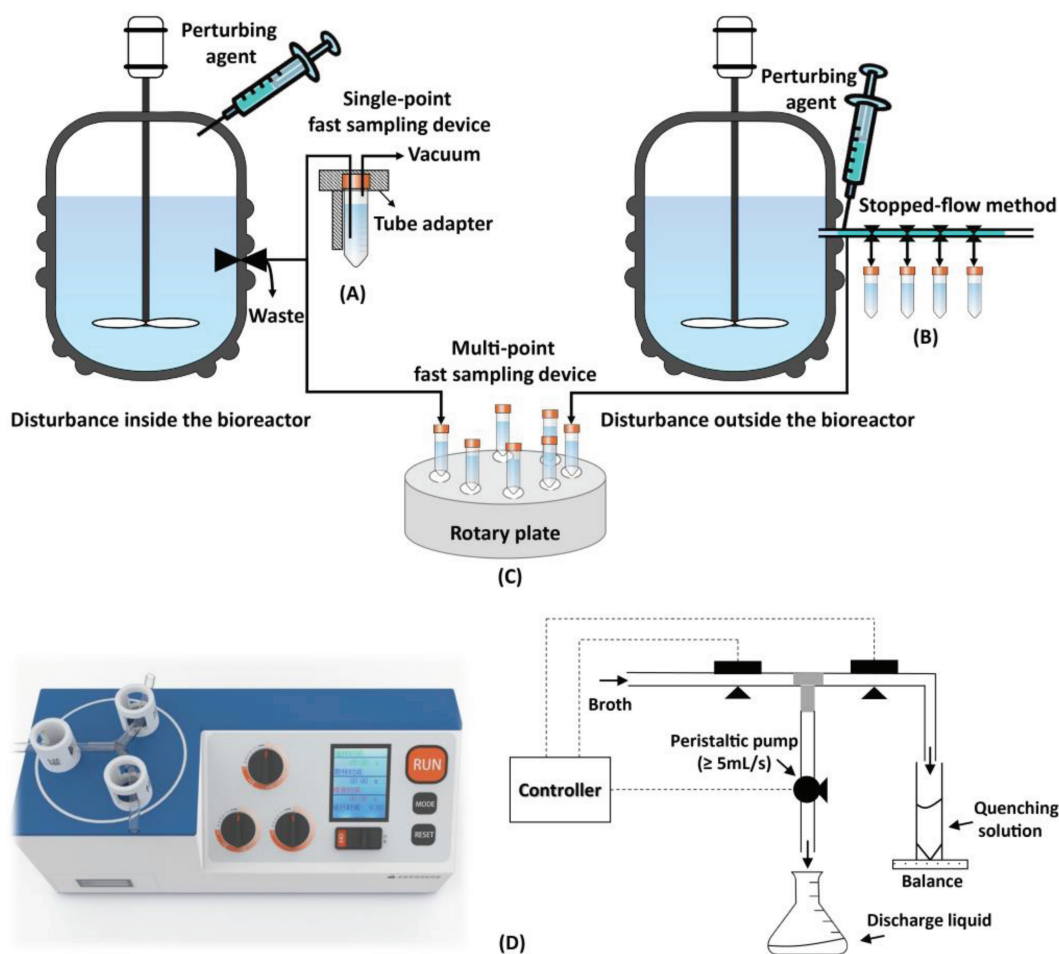


FIGURE 44.2 Representative rapid sampling devices for metabolic engineering applications. (A) Single-point fast sampling device; (B) 'stopped-flow' fast sampling device; (C) multi-point fast sampling devices; (D) in-house rapid sampling device (left) and its working procedure (right).

obtain metabolic snapshots in diverse fermentations, with minimal error resulting from the sampling process.^{43,51–57}

To enable immediate quenching of all enzymatic activities and freeze all metabolites with minimal loss, conventional centrifugation-based quenching, and washing methods have been developed and used for decades in fermentations with bacteria, yeasts, and filamentous fungi. The most common quenching protocol employs cold methanol at a low temperature, e.g., less than -40°C ; samples were obtained with the rapid sampling device by rapidly withdrawing a certain amount of broth from the bioreactor into a tube containing the quenching solution. Afterwards, cold centrifugation allows the separation of cells and the supernatant. Nonetheless, it has been reported that this caused serious leakage and/or cold shock for some microorganisms during the sampling process.^{58–63} In addition to metabolite leakage during the quenching and separation, incomplete removal of supernatant from cell pellet/cake and metabolite coprecipitation will aggravate the misestimation of the intracellular metabolite amount.⁶⁴ Different strategies have been proposed to account for this bias,⁶⁵ such as (i) preserve cell integrity by adding cryoprotective, osmoprotective, or pH-stabilizing agents, (ii) quantify and correct the leakage by additional analysis of the quenching supernatant sample after cell separation, and (iii) completely circumvent the leakage by simultaneous quenching and extraction of the entire metabolome of the sample. To further reduce metabolite leakage and enhance washing efficiency, a cold filtration-based washing method has been developed to reduce the exposure time to the quenching liquid, and for efficient removal of extracellular substrates and products.⁶⁶ For example, Douma, de Jonge⁶⁶ used this method for the first time allowing to measure the intracellular levels of the precursor phenylacetic acid and the product penicillin G, compounds of which the extracellular concentrations were 3–4 orders of magnitude higher than their intracellular counterparts within the penicillin biosynthesis pathway.

To achieve complete extraction of intracellular metabolites, a multitude of extraction methods such as multiple freezing-thawing in methanol, hot water, hot methanol, boiling ethanol, acidic acetonitrile-methanol, chloroform-methanol (un)buffered ethanol, perchloric acid, and alkaline methods have been developed and evaluated for metabolite extraction from different host cells.^{67–70} For example, for filamentous fungi and yeasts, the use of boiling ethanol for extraction is preferred over conventional procedures that involve strong acid or alkali reagents, which often lead to incomplete extraction and metabolite instability; better results are achieved in terms of recovery and stability of metabolites.^{71,72} For *Escherichia coli*, multiple freeze-thaw cycles using 100% methanol at -48°C are recommended for the extraction of metabolites.⁷⁰ For mammalian cells, the best performance is observed for a wide range of metabolites when two 100% methanol extractions followed by a water extraction are used.⁷³ However, due to different metabolite properties (polarity, molecular weight) and different cellular envelop structures, complementary extractions would be necessary to

maximize the range of metabolites and attain a global metabolite profile from a single sample.

44.2.2 THE STABLE ISOTOPE DILUTION THEORY

After performing a well-established fast sampling, quenching, and extraction protocol, the cellular metabolism can be frozen and metabolites extracted to facilitate further analysis. A range of analytical techniques can be used to measure intracellular metabolite concentrations in the obtained cell extracts. Due to the simultaneous identification and quantification of a large number of metabolites with high selectivity, adequate sensitivity, and minimal sample use (e.g., 5–10 μL vs. 100 μL or more for enzyme assays), high-throughput mass spectrometric techniques are often preferred to traditional enzymatic and chromatographic methods.⁷⁴ However, prior to metabolite determination, several factors affecting absolute quantitation should be addressed. Quantitative metabolite profiling is often hampered by biased mass spectrometry-based analyses caused by matrix effects, the degradation of metabolites and metabolite leakage during sample preparation, operator-to-operator variations and unexpected variation in instrument responses.⁴³ Consequently, mass spectrometry-based analysis of the metabolites cannot be directly used without validation, and metabolite recoveries in the extraction procedure require checking via laborious standard addition experiments for each metabolite of interest.

To address the problems mentioned above in sample preparation and MS-based analysis, the isotope dilution technique has been proposed to correct most aspects of analytical biases.⁷⁵ The stable isotope dilution theory states that the relative signal intensity in an MS of two analytes that are chemically identical but of different stable isotope compositions, such as ^{13}C and ^{15}N skeleton elements, distinguishable in a mass analyzer, are a true representation of the relative abundance of the two analytes in a sample.⁴³ Therefore, degradation during sample preparation, variations in instrumental response, and ion suppression effects in mass spectrometry can be compensated.⁷⁴ This technique has been widely used to generate accurate and quantitative metabolomics data.^{43,51–54,74,76–82} Nevertheless, the availability of labeled intracellular metabolites is scarce, and chemical synthesis of the isotope of interest is highly expensive and time-consuming. An appropriate way is to use microorganisms to synthesize these uniformly- ^{13}C -labeled equivalents. In general, primary metabolites in the central metabolic pathways are relatively easy to obtain, while secondary metabolites in the production pathway need to be artificially enriched. For example, Wu, Mashego⁷⁴ obtained uniformly- ^{13}C -labeled cell extracts for each intracellular metabolite of interest by cultivating *S. cerevisiae* in a fed-batch mode on fully uniformly- ^{13}C -labeled substrates. However, for the enrichment of intermediates in the penicillin pathway, as shown in Figure 44.3, Wang, Chu⁴³ prepared uniformly- ^{13}C -labeled cell extracts by cultivating *P. chrysogenum* in an exponential fed-batch fermentation with fully uniformly- ^{13}C -labeled substrates at the optimal growth rate of 0.03 h^{-1} , for which it was previously shown that the penicillin

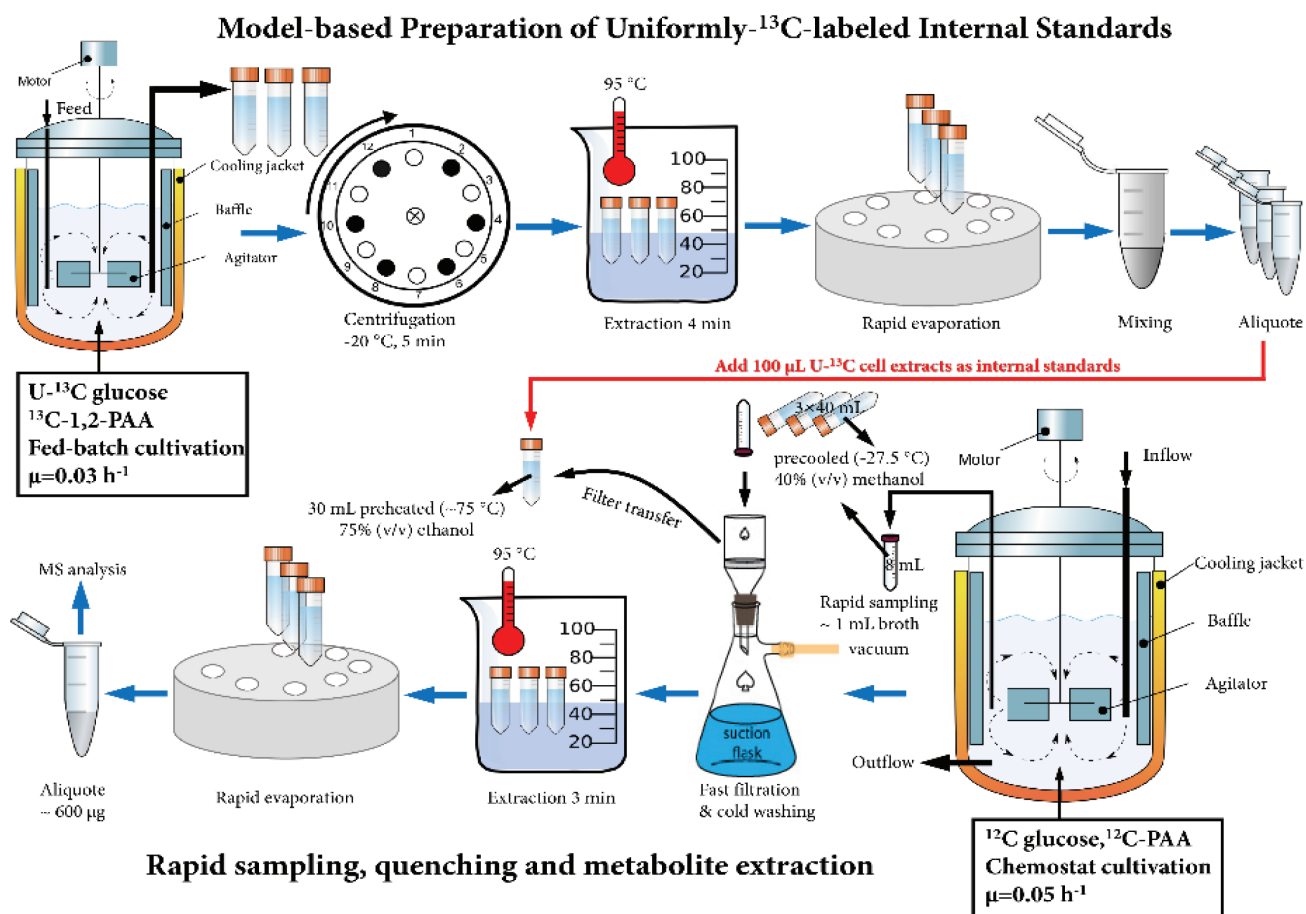


FIGURE 44.3 Preparation of uniformly ¹³C-labeled cell extracts as internal standards and the flowchart of a well-established fast sampling, quenching, and metabolite extraction procedure for quantitative metabolomics of *P. chrysogenum*. (Reproduced from Wang, Chu⁴³ with permission from Elsevier.)

productivity was maximized under glucose-limited conditions. Based on a well-established fast sampling, quenching, and extraction protocol, the cultivated U-¹³C-labeled biomass yielded essentially the whole *P. chrysogenum* metabolome and, in principle, provided U-¹³C-labeled internal standards for each intracellular metabolite of interest.⁸³

44.3 METABOLOMICS-ASSISTED SYSTEMS METABOLIC ENGINEERING

Cell factories with high productivity and yield at large scale require appropriate distribution of cellular resources toward biomass growth, product formation, and cellular maintenance, which then provides a new paradigm in metabolic engineering to manipulate and optimize metabolic pathways. Systems metabolic engineering was born by incorporating concepts and techniques of systems biology, synthetic biology and evolutionary engineering. This, to a great extent, accelerates pathway modification or the creation of new metabolic enzymes for the optimal production of target products.⁸⁴

Metabolomics, as the newest omics tool among the systems biology tools, has been advocated to identify and interpret genotype-phenotype associations in model organisms.¹⁵

Especially, the recent marriage of metabolomics and synthetic biology expedites the application of systems metabolic engineering tools toward strain improvement and process intensification.⁸⁵ For example, a recent and highly topical study of metabolic pathways based on metabolomics focused on the increased tolerance of *S. cerevisiae* to inhibitors in lignocellulosic hydrolysates during bioethanol production.⁸⁶ In this study, metabolite profiling was used to examine the effect of acetic acid on xylose fermentation and to identify genes for improving organic acid tolerance. The results revealed acetic acid attenuates the non-oxidative pentose phosphate pathway (PPP). Therefore, overexpression of the PPP-related enzyme (transaldolase or transketolase) conferred ethanol productivity in the presence of both acetic and formic acid.⁸⁶ In addition, tracking metabolite labeling from stable isotope tracers can reveal pathway activities.¹¹ For instance, de Jonge, Buijs⁸⁷ imposed intermittent feeding on chemostat cultures of a penicillin G-producing *P. chrysogenum* strain to simulate substrate gradients present in a large-scale fermentation and estimated the intracellular flux changes based on dynamic ¹³C mass isotope measurements using a novel hybrid modeling approach. The results revealed that the turnover rate of storage carbohydrates (e.g., trehalose, mannitol, glycogen) in this high-yielding

P. chrysogenum strain is increased under dynamic cultivation conditions and may partly contribute to the observed decrease in penicillin productivity.⁸⁷ Trehalose cycling has been regarded as a double-edged sword in the *P. chrysogenum* strain, which is instrumental in maintaining a metabolically balanced state. Yet, it consumes extra amounts of ATP for the periodic formation and breakdown of trehalose in response to extracellular glucose perturbations.^{87,88} To address this, in a follow-up study, Wang, Zhao⁵³ for the first time constructed *P. chrysogenum* mutant strains with altered trehalose metabolism; the results revealed that trehalose is indispensable to maintaining the balanced metabolic state and thus high penicillin production capacity under both steady state and feast/famine conditions.⁸⁹ Cells lacking intact trehalose would become more sensitive to repeated extracellular glucose perturbations, which can aggravate the loss of the penicillin production capacity, manifesting in an almost 40% more reduction in trehalose-mutant strains.⁸⁹ Dynamic metabolomics has been accelerating learning step within the DBTL cycle for bioproduction capability, and examples for central metabolites, organic acids, aromatic compounds, and terpenoids have been recently reviewed by Vavricka, Hasunuma.⁹⁰

In industrial settings, adaptation of cells to environmental changes requires dynamic interactions between metabolic and regulatory networks,⁹¹ and thus it is of utmost importance to know why the optimum production performance is not reached in practice and where regulatory

limitations really are.⁹² Mathematical models serving as a tool for understanding cellular metabolism and physiology have been used to define optimal fermentation conditions, as well as direct the genetic changes toward achieving a desired producer strain or cell line.⁹³ As discussed previously, large-scale stoichiometric models, e.g., genome-scale metabolic models, although they provide informative clues on the phenotypes of different deletion mutants in silico using linear optimization, are usually not capable of describing cellular dynamics and regulatory architecture upon environmental changes, which is, however, the reality at the large-scale condition. In contrast, kinetic models can provide a dynamic picture of specific cellular processes by combining kinetics with the known stoichiometry of metabolic pathways. Nevertheless, developing a detailed kinetic model is often constrained by the availability of data sources under industrial-relevant scenarios. To bridge this gap, a reduced kinetic model that focuses on the key metabolic pathways leading to central metabolites (or precursors), products, energy, storage pools, and maintenance can be formulated while preserving enough dynamic features.⁹⁴

A recent leading example has been the establishment of a 9-pool metabolic structured kinetic model that allows the description of dynamics of cellular growth and product formation by *P. chrysogenum* at timescales of seconds to days.¹³ In this study, based on time hierarchy and metabolite properties, as shown in Figure 44.4, the 9-pool model was developed with five lumped intracellular metabolite

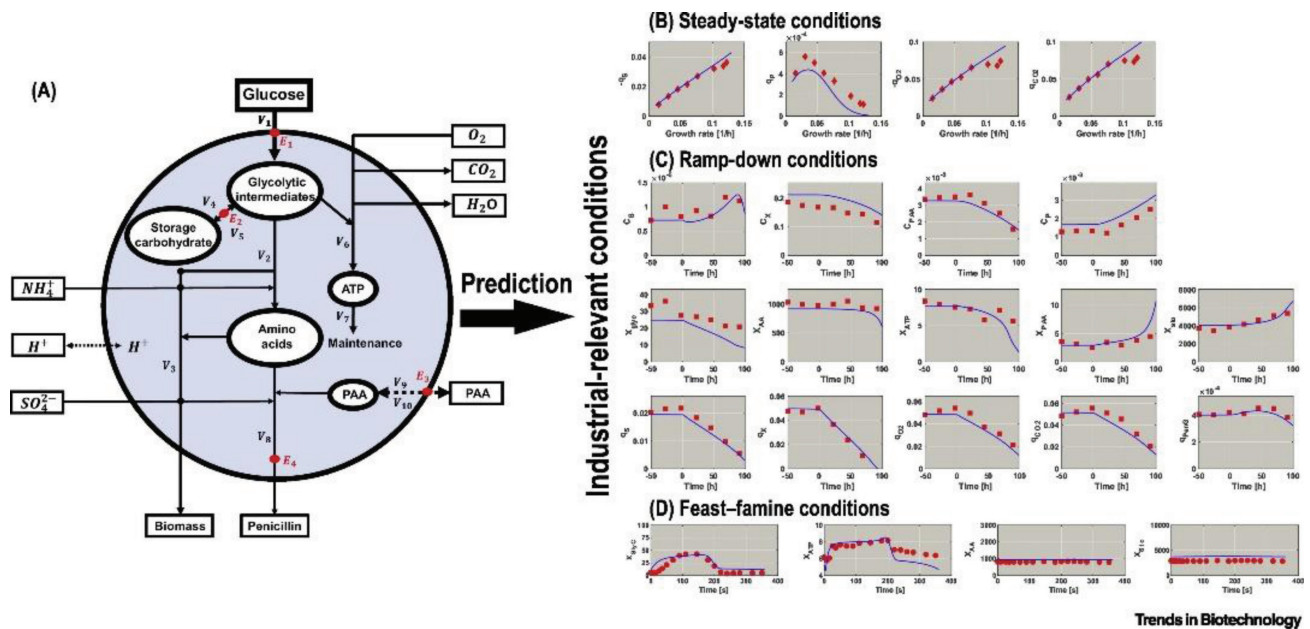


FIGURE 44.4 Overview of the Nine-Pool Model for *Penicillium chrysogenum*. (A) Lumped metabolic pools, such as glycolytic intermediates, storage carbohydrates, and amino acids, are defined by metabolite properties and turnover timescales. The final model contains five lumped intracellular metabolite pools (glycolytic intermediates, amino acids, ATP, PAA, and storage carbohydrates), four enzyme (capacity) pools (glucose uptake, PAA export, penicillin conversion, and storage conversion), and ten extracellular components, connected via ten intracellular reactions. Comparison of model predictions and experimental data: (B) as a function of the specific growth rate under chemostat conditions; (C) as a function of time during steady state (–50 to 0 h) and ramp phases (0 to 100 h); (D) under a complete feast–famine cycle of 360 s using block-wise feeding (36 s on, 324 s off). Extracellular c_i (mol/kg), intracellular X_i ($\mu\text{mol/gDW}$), and specific rates q_i (mol/CmolX/h). Experimental data (red symbols) and simulated result (blue lines) predicted by the nine-pool model. Abbreviation: PAA, phenylacetic acid. (Reproduced from Wang et al.³⁶ with permission from Elsevier.)

pools (glycolytic intermediates, amino acids, ATP, PAA, and storage carbohydrates), four enzyme (capacity) pools (glucose uptake, PAA export, penicillin conversion, and storage conversion), and ten extracellular components, connected via ten intracellular reactions. This established kinetic model can fulfill accurate predictions of both extracellular specific rates and lumped intracellular metabolite pools under industrially relevant conditions (Figure 44.4), and more importantly, it can reproduce the productivity loss under highly dynamic conditions.⁹⁵ Moreover, this 9-pool model was established with the mindset of future integration in a CFD framework at the very beginning. Hence, detailed explanations will be presented in the next section to show the power of the combination of CRD and CFD for bioprocess description and evaluation.

44.4 THROUGH THE ORGANISM'S EYES: GETTING CLOSER TO THE WHOLE PICTURE

Table 44.2 gives the mixing times of different types of large-scale bioreactors, ranging from tens to hundreds of seconds, which is usually longer than the timescales of biochemical reactions in the cell (Table 44.1). Consequently, nonideal mixing and mass transfer limitations are prone to result in spatiotemporal environmental gradients of, e.g., substrate, dissolved oxygen, and protons in large-scale bioreactors.

Although experimental scale-down studies have shown that the heterogenous environment at large scale potentially impacts the metabolic response and thus process performance of the cell,²³ there are few studies aiming to quantify this impact, for example, by combining dynamic metabolic models with CFD simulations. In particular, CFD simulations can be used to assess the environment from the perspective of the organism, defining their trajectories in the industrial bioreactor and determining the temporal variations in the environment they observe along this trajectory, often referred to as a lifeline. Such simulations offer great potential for integrating transport dynamics and metabolic dynamics in fermentation systems.⁹⁶ Simulation methods in which the trajectories of individual cells, or groups of cells, are determined are referred to as Euler-Lagrange simulations. This approach treats the fluid phase as a continuum and the dispersed biophase, e.g., microbial cells, as virtual particles, for which the trajectory is resolved by solving the equations of motion for each individual.⁹⁷ For example, the pioneering work by Lapin, Muller⁹⁸ describes population behavior as the outcome of the interaction between the intracellular state of individual cells, with the local extracellular availability of substrates, transported by the turbulent flow in the reactor. The computational results showed a dramatic loss of synchronization of temporal oscillations in glycolytic metabolites at the single-cell level in the presence of a spatially heterogeneous glucose concentration field. Further, in order to verify this integration method, Lapin and Schmid⁹⁹ modeled the dynamics of *Escherichia*

TABLE 44.2
Reported 95% Mixing Times in Industrial-Scale Bioreactors

Type of Reactors	Cell Lines	Mixing Time(s)
Cell culture		
5-L STR	CHO	2-5
8.5-L STR	Plant cells	3.6
11-L STR Helical ribbon	Plant cells	18-25
20-L STR	CHO	20-80
8 m ³ STR	Namalwa cells	40-200
10 m ³ STR ^a	Plant cells	20-200
12 m ³ STR	Mammalian cells	120-360
10-L STR with spin filter	CHO	120
Hydrofoil impeller, 20 rpm		
250-L STR with spin filter		
Hydrofoil impeller, 80 rpm	CHO	120
250-L STR with spin filter		
Pitched blade impeller, 80 rpm	CHO	1620
1 m ³ STR with spin filter		
Hydrofoil impeller/mixing through spin filter	CHO	3120
15-L bubble column	Plant roots	2400
10 m ³ Airlift ^a	Plant cells	200-1000
Microbial cultures		
12 m ³ STR, equipped with 3 Rushton-type impellers	Microorganisms	10-50
12 m ³ STR, equipped with 3 Scaba-type impellers	Microorganisms	10-30
30 m ³ STR, equipped with 3 Rushton-type impellers	Microorganisms	125-250
30 m ³ STR, equipped with 3 Scaba-type impellers	Microorganisms	70-110
2 m ³ Bubble column	Microorganisms	18
2 m ³ Airlift	Microorganisms	80
4 m ³ Airlift tower loop	Baker's yeast	100-175
40 m ³ Bubble column	Microorganisms	80
40 m ³ Airlift	Microorganisms	101
150 m ³ Bubble column	Baker's yeast	10-1000

^a Estimated.

Source: Adapted from Wang et al.¹⁰² with permission of John Wiley & Sons.

coli populations in the three-dimensional turbulent flow field of a stirred-tank reactor. In this study, a phosphotransferase system for the sugar uptake was incorporated into the cellular kinetic model, and the results revealed that the activity of the sugar uptake system is dependent on both the local glucose concentration and the ratio of intracellular phosphoenolpyruvate and pyruvate, which is as a function of the lifeline of the individual cell in the large-scale bioreactor. In the literature, there are emerging applications of CFD-CRD models to assess spatially resolved bioreactor performance from the cellular perspective and/or including structured kinetic models, which has been recently reviewed in Wang, Haringa.³⁶

To allow a more detailed kinetic description of the cell, incorporating more biochemical mechanisms is desired,

while computational tractability and computation time should be taken into account considering the application toward hydrodynamic coupling. Recently, a leading example has been the CFD simulation of an industrial *P. chrysogenum* fermentation with a coupled 9-pool metabolic model.¹⁰⁰ In this study, the effect of substrate heterogeneity on the metabolic response of *P. chrysogenum* in industrial bioreactors was assessed, and the simulation results showed a 33% loss in production rate and yield under chemostat conditions while also showing good agreement with industrial production rate dynamics under fed-batch conditions. Meanwhile, the spontaneous emergence of population heterogeneity in the glucose uptake capacity was observed in the model, and both extracellular and intracellular metabolic

fluctuations at seconds to days timescales were recorded (Figure 44.5). Furthermore, this computational framework can provide suggestions for improving a cell factory because it serves to comprehend, predict, and evaluate the effects of adding, removing, or modifying molecular components and/or pathways.³⁶ Moreover, direct suggestions on the design of the bioreactor and fermentation process can be achieved. For example, the original feed point location is at the top of the fermentor in industrial-scale penicillin fermentation, which induces substrate gradients along with three representative metabolic regimes, e.g., glucose excess, limitation, and starvation.²² The *in silico* optimization of moving the feedpoint from the top to the middle increases the volume operating under favorable production conditions, and

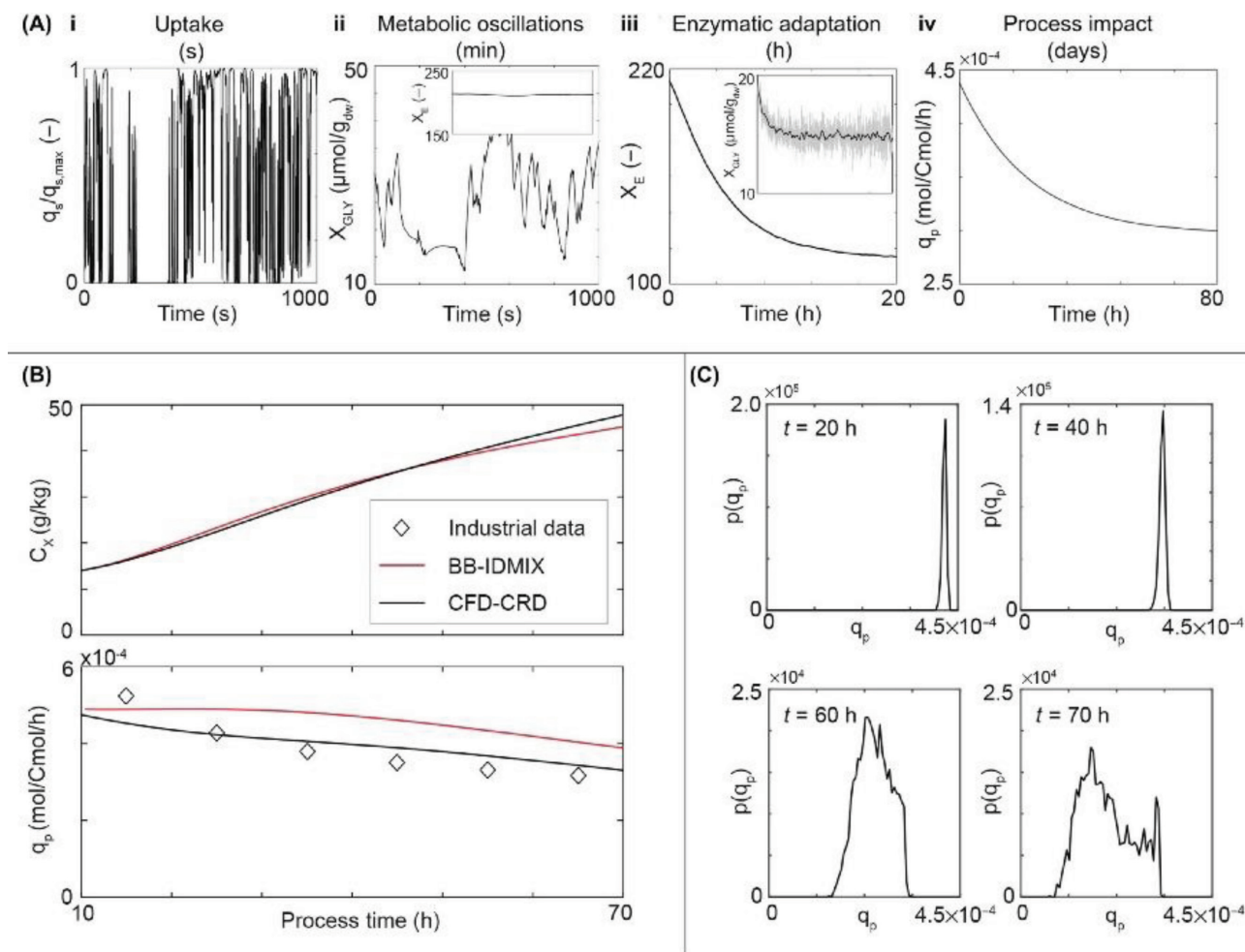


FIGURE 44.5 Results of a coupled CFD-CRD simulation for a penicillin production process. (A) Illustration of process response at different timescales. Extracellular fluctuations in substrate concentration cause fluctuations in substrate uptake rate (i) on the second timescale, leading to metabolic variations on the minute timescale (ii); enzyme levels are constant at this timescale (ii, inset). On an hour timescale, metabolic fluctuations cause enzyme-level adaptation (iii). These, in turn, can affect metabolic fluctuations (inset; rolling average in black, fluctuations in gray). Finally, enzyme adaptation changes the penicillin production rate over the full process time (iv). (B) Performance of CFD-CRD in an industrial fed-batch process compared with a black box, ideal-mixed model (BB-IDMIX). (C) Due to differences observed early during the process, individual metabolic responses lead to divergence in the population as a function of time; after 20 h, all organisms have nearly the same production rate, while after 60 h, a wider distribution is observed (sampled from 2500 tracked organisms). (Reproduced from Wang et al.³⁶ with permission from Elsevier.)

reduces glucose excess/starvation zones, which eventually contributes to improving production performance.¹⁹ In addition, the acquired fluctuation statistics can be used to design representative scale-down simulators.⁹⁶

44.5 CONCLUDING REMARKS

Despite the central issue of scale-up effects during bioprocess development, there appears to be no unequivocal bioprocess scale-up principle in the past two decades, just as Arthur Humphrey commented that scale-up is still an art, not a science.¹⁰¹ Indeed, no longer are Rushton impellers the answer, and no longer are we concerned only with maintaining the same volumetric mass transfer coefficient (K_La).¹⁰¹ An industrial-scale bioprocess is a complex multi-scale system where a small perturbation on one scale (e.g., genetic scale) could give rise to considerable changes on another scale (e.g., cellular scale and bioreactor scale). Hence, how to deal with the complex interplay between the cellular machinery and the extracellular environment challenges both academic researchers and industrial practitioners.

With the great strides in computer science and systems metabolic engineering tools, an ever-increasing understanding of the relationships between cellular behaviors and the surrounding environments during bioprocess development has been achieved. This eventually opens avenues for developing more robust cell lines and reproducible bioprocesses. Among the omics diagnostic technologies, metabolomics provides functional readouts of cellular function and interaction with their surroundings, thus accelerating the learning step in the DBTL cycle for enhanced bioproduction capability. More importantly, quantitative metabolomics can be used to establish a highly predictive metabolic model, which serves to understand, predict, and optimize the properties and behaviors of the cell factory in a dynamic environment. Furthermore, as long as the metabolically structured model is constructed with the mindset of coupling it with the CFD model, the interaction between hydrodynamics and metabolic dynamics in industrial-scale fermentation processes can be evaluated through the organism's eyes. This coupled full-scale predictive model can guide decision-making for intelligent biomanufacturing and fulfills the ambitions of 'Industry 4.0' toward digitalization and automation.

SUMMARY

As the youngest of the quartet of systems biology tools alongside genomics, transcriptomics, and proteomics, metabolomics provides an immediate and dynamic recording of cells in response to genetic and/or environmental perturbations. Metabolomics study accelerates learning steps within the iterative DBTL cycle for enhancing bioproduction capability. The associations between biological networks and environmental factors facilitate predictive modeling of cellular response, which is the basis for industrial application. This chapter presents an update on the

metabolomics-driven biosystems engineering and bioprocess design principle from the metabolic perspective of organisms. Along with the introduction of the isotope dilution mass spectrometry (ID-MS) method to the fast sampling, quenching, and extraction protocol for quantitative metabolomics, metabolomics-assisted engineering biology and the establishment of metabolically structured models are highlighted. Furthermore, a computational framework based on a coupled metabolic-hydrodynamic approach is advocated to assess the interlocking architectures between environmental and biological networks in large-scale bioprocesses and provide suggestions toward bioreactor evaluation, scale-down, and optimization.

ACKNOWLEDGMENTS

This work was financially supported by the National Natural Science Foundation of China (Grant no. 31900073, 21978085), the Science and Technology Commission of Shanghai Municipality (Grant no. 19ZR1413600), Shanghai Rising-Star Program (21QA1402400) and the 111 Project (Grant no. B18022).

REFERENCES

- Smolke CD, Silver PA. Informing biological design by integration of systems and synthetic biology. *Cell*. 2011;144:855–859.
- Nielsen J, Fussenegger M, Keasling J, et al. Engineering synergy in biotechnology. *Nat Chem Biol*. 2014;10:319–322.
- Yugi K, Kuroda S. Metabolism-centric trans-omics. *Cell Syst*. 2017;4:19–20.
- Allen J, Davey HM, Broadhurst D, et al. High-throughput classification of yeast mutants for functional genomics using metabolic footprinting. *Nat Biotechnol*. 2003;21:692–696.
- Damiani C, Gaglio D, Sacco E, Alberghina L, Vanoni M. Systems metabolomics: from metabolomic snapshots to design principles. *Curr Opin Biotechnol*. 2020;63:190–199.
- van Winden WA, Heijnen JJ, Verheijen PJT, Grievink J. A priori analysis of metabolic flux identifiability from C-13-labeling data. *Biotechnol Bioeng*. 2001;74:505–516.
- Zamboni N, Sauer U. Novel biological insights through metabolomics and 13C-flux analysis. *Curr Opin Microbiol*. 2009;12:553–558.
- Sauer U. Metabolic networks in motion: 13C-based flux analysis. *Mol Syst Biol*. 2006;2:62.
- Zamboni N, Saghatelian A, Patti GJ. Defining the metabolome: Size, flux, and regulation. *Mol Cell*. 2015;58:699–706.
- Allen DK, Young JD. Tracing metabolic flux through time and space with isotope labeling experiments. *Curr Opin Biotechnol*. 2020;64:92–100.
- Jang C, Chen L, Rabinowitz JD. Metabolomics and isotope tracing. *Cell*. 2018;173:822–837.
- Nikerel IE, van Winden WA, Verheijen PJ, Heijnen JJ. Model reduction and a priori kinetic parameter identifiability analysis using metabolome time series for metabolic reaction networks with linlog kinetics. *Metab Eng*. 2009;11:20–30.
- Tang W, Deshmukh AT, Haringa C, et al. A 9-pool metabolic structured kinetic model describing days to seconds dynamics of growth and product formation by *Penicillium chrysogenum*. *Biotechnol Bioeng*. 2017;114:1733–1743.

14. Toya Y, Shimizu H. Flux analysis and metabolomics for systematic metabolic engineering of microorganisms. *Biotechnol Adv.* 2013;31:818–826.
15. Zampieri M, Sauer U. Metabolomics-driven understanding of genotype-phenotype relations in model organisms. *Curr Opin Syst Biol.* 2017;6:28–36.
16. Diether M, Nikolaev Y, Allain FH, Sauer U. Systematic mapping of protein-metabolite interactions in central metabolism of *Escherichia coli*. *Mol Syst Biol.* 2019;15:e9008.
17. Kochanowski K, Gerosa L, Brunner SF, Christodoulou D, Nikolaev YV, Sauer U. Few regulatory metabolites coordinate expression of central metabolic genes in *Escherichia coli*. *Mol Syst Biol.* 2017;13:903.
18. Hackett SR, Zanolli VR, Xu W, et al. Systems-level analysis of mechanisms regulating yeast metabolic flux. *Science.* 2016;354:aaf2786.
19. Wang G, Haringa C, Tang W, et al. Coupled metabolic-hydrodynamic modeling enabling rational scale-up of industrial bioprocesses. *Biotechnol Bioeng.* 2020;117:844–867.
20. Larsson G, Törnkvist M, Wernersson ES, Trägårdh C, Noorman H, Enfors S-O. Substrate gradients in bioreactors: Origin and consequences. *Bioprocess Eng.* 1996;14:281–289.
21. Bylund F, Collet E, Enfors S-O, Larsson G. Substrate gradient formation in the large-scale bioreactor lowers cell yield and increases by-product formation. *Bioprocess Eng.* 1998;18:171–180.
22. Haringa C, Tang W, Deshmukh AT, et al. Euler-Lagrange computational fluid dynamics for (bio)reactor scale down: An analysis of organism lifelines. *Eng Life Sci.* 2016;16:652–663.
23. Lara AR, Galindo E, Ramirez OT, Palomares LA. Living with heterogeneities in bioreactors: Understanding the effects of environmental gradients on cells. *Mol Biotechnol.* 2006;34:355–381.
24. Käß F, Junne S, Neubauer P, Wiechert W, Oldiges M. Process inhomogeneity leads to rapid side product turnover in cultivation of *Corynebacterium glutamicum*. *Microb Cell Fact.* 2014;13:6.
25. Enfors SO, Jahic M, Rozkov A, et al. Physiological responses to mixing in large scale bioreactors. *J Biotechnol.* 2001;85:175–185.
26. Bhargava S, Nandakumar MP, Roy A, Wenger KS, Marten MR. Pulsed feeding during fed-batch fungal fermentation leads to reduced viscosity without detrimentally affecting protein expression. *Biotechnol Bioeng.* 2003;81:341–347.
27. Bhargava S, Wenger KS, Marten MR. Pulsed addition of limiting-carbon during *Aspergillus oryzae* fermentation leads to improved productivity of a recombinant enzyme. *Biotechnol Bioeng.* 2003;82:111–117.
28. Song H-S, DeVilbiss F, Ramkrishna D. Modeling metabolic systems: The need for dynamics. *Current Opinion in Chemical Engineering.* 2013;2:373–382.
29. Srinivasan S, Cluett WR, Mahadevan R. Constructing kinetic models of metabolism at genome-scales: A review. *Biotechnol J.* 2015;10:1345–1359.
30. Douma RD, Verheijen PJ, de Laat WT, Heijnen JJ, van Gulik WM. Dynamic gene expression regulation model for growth and penicillin production in *Penicillium chrysogenum*. *Biotechnol Bioeng.* 2010;106:608–618.
31. Deshmukh AT, Verheijen PJT, Maleki Seifar R, Heijnen JJ, van Gulik WM. In vivo kinetic analysis of the penicillin biosynthesis pathway using PAA stimulus response experiments. *Metab Eng.* 2015;32:155–173.
32. Andreozzi S, Miskovic L, Hatzimanikatis V. iSCHRUNK – In silico approach to characterization and reduction of uncertainty in the kinetic models of genome-scale metabolic networks. *Metab Eng.* 2016;33:158–168.
33. Kesten D, Kummer U, Sahle S, Hubner K. A new model for the aerobic metabolism of yeast allows the detailed analysis of the metabolic regulation during glucose pulse. *Biophys Chem.* 2015;206:40–57.
34. Smallbone K, Mendes P. Large-scale metabolic models: From reconstruction to differential equations. *Ind Biotechnol.* 2013;9:179–184.
35. Link H, Christodoulou D, Sauer U. Advancing metabolic models with kinetic information. *Curr Opin Biotechnol.* 2014;29:8–14.
36. Wang G, Haringa C, Noorman H, Chu J, Zhuang Y. Developing a computational framework to advance bioprocess scale-up. *Trends Biotechnol.* 2020;38:846–856.
37. Heijnen JJ. Approximative kinetic formats used in metabolic network modeling. *Biotechnol Bioeng.* 2005;91:534–545.
38. Volkova S, Matos MRA, Mattanovich M, Marin de Mas I. Metabolic modelling as a framework for metabolomics data integration and analysis. *Metabolites.* 2020;10.
39. Wang J, Wang C, Liu H, Qi H, Chen H, Wen J. Metabolomics assisted metabolic network modeling and network wide analysis of metabolites in microbiology. *Crit Rev Biotechnol.* 2018;38:1106–1120.
40. Bennett BD, Kimball EH, Gao M, Osterhout R, Van Dien SJ, Rabinowitz JD. Absolute metabolite concentrations and implied enzyme active site occupancy in *Escherichia coli*. *Nat Chem Biol.* 2009;5:593–599.
41. Niebel B, Leupold S, Heinemann M. An upper limit on Gibbs energy dissipation governs cellular metabolism. *Nat Metab.* 2019;1:125–132.
42. Link H, Fuhrer T, Gerosa L, Zamboni N, Sauer U. Real-time metabolome profiling of the metabolic switch between starvation and growth. *Nat Methods.* 2015;12:1091–1097.
43. Wang G, Chu J, Zhuang Y, van Gulik W, Noorman H. A dynamic model-based preparation of uniformly-(13) C-labeled internal standards facilitates quantitative metabolomics analysis of *Penicillium chrysogenum*. *J Biotechnol.* 2019;299:21–31.
44. van Gulik WM. Fast sampling for quantitative microbial metabolomics. *Curr Opin Biotechnol.* 2010;21:27–34.
45. Canelas AB, van Gulik WM, Heijnen JJ. Determination of the cytosolic free NAD/NADH ratio in *Saccharomyces cerevisiae* under steady-state and highly dynamic conditions. *Biotechnol Bioeng.* 2008;100:734–743.
46. Nasution U, van Gulik WM, Kleijn RJ, van Winden WA, Proell A, Heijnen JJ. Measurement of intracellular metabolites of primary metabolism and adenine nucleotides in chemostat cultivated *Penicillium chrysogenum*. *Biotechnol Bioeng.* 2006;94:159–166.
47. Nasution U, van Gulik WM, Proell A, van Winden WA, Heijnen JJ. Generating short-term kinetic responses of primary metabolism of *Penicillium chrysogenum* through glucose perturbation in the bioscope mini reactor. *Metab Eng.* 2006;8:395–405.
48. Taymaz-Nikerel H, de Mey M, Ras C, et al. Development and application of a differential method for reliable metabolome analysis in *Escherichia coli*. *Anal Biochem.* 2009;386:9–19.
49. Schadel F, Franco-Lara E. Rapid sampling devices for metabolic engineering applications. *Appl Microbiol Biotechnol.* 2009;83:199–208.

50. Hiller J, Franco-Lara E, Papaioannou V, Weuster-Botz D. Fast sampling and quenching procedures for microbial metabolic profiling. *Biotechnol Lett.* 2007;29:1161–1167.
51. Wang G, Wang X, Wang T, et al. Comparative fluxome and metabolome analysis of formate as an auxiliary substrate for penicillin production in glucose-limited cultivation of *Penicillium chrysogenum*. *Biotechnol J.* 2019;14:e1900009.
52. Wang G, Zhao J, Haringa C, et al. Comparative performance of different scale-down simulators of substrate gradients in *Penicillium chrysogenum* cultures: The need of a biological systems response analysis. *Microb Biotechnol.* 2018;11:486–497.
53. Wang G, Zhao JF, Wang XX, et al. Quantitative metabolomics and metabolic flux analysis reveal impact of altered trehalose metabolism on metabolic phenotypes of *Penicillium chrysogenum* in aerobic glucose-limited chemostats. *Biochem Eng J.* 2019;146:41–51.
54. Li C, Shu W, Wang S, et al. Dynamic metabolic response of *Aspergillus niger* to glucose perturbation: Evidence of regulatory mechanism for reduced glucoamylase production. *J Biotechnol.* 2018;287:28–40.
55. Cao W, Wang G, Lu H, et al. Improving cytosolic aspartate biosynthesis increases glucoamylase production in *Aspergillus niger* under oxygen limitation. *Microb Cell Fact.* 2020;19:81.
56. Sui YF, Schutze T, Ouyang LM, et al. Engineering cofactor metabolism for improved protein and glucoamylase production in *Aspergillus niger*. *Microb Cell Fact.* 2020;19:198.
57. Liu X, Wang T, Sun X, et al. Optimized sampling protocol for mass spectrometry-based metabolomics in *Streptomyces*. *Bioresour Bioprocess.* 2019; 6:1–12
58. Bolten CJ, Kiefer P, Letisse F, Portais JC, Wittmann C. Sampling for metabolome analysis of microorganisms. *Anal Chem.* 2007;79:3843–3849.
59. Canelas AB, Ras C, ten Pierick A, van Dam JC, Heijnen JJ, Van Gulik WM. Leakage-free rapid quenching technique for yeast metabolomics. *Metabolomics.* 2008;4:226–239.
60. de Jonge LP, Douma RD, Heijnen JJ, van Gulik WM. Optimization of cold methanol quenching for quantitative metabolomics of *Penicillium chrysogenum*. *Metabolomics.* 2012;8:727–735.
61. Kim S, Lee DY, Wohlgemuth G, Park HS, Fiehn O, Kim KH. Evaluation and optimization of metabolome sample preparation methods for *Saccharomyces cerevisiae*. *Anal Chem.* 2013;85:2169–2176.
62. Wellerdiek M, Winterhoff D, Reule W, Brandner J, Oldiges M. Metabolic quenching of *Corynebacterium glutamicum*: Efficiency of methods and impact of cold shock. *Bioprocess Biosyst Eng.* 2009;32:581–592.
63. Wittmann C, Kromer JO, Kiefer P, Binz T, Heinzle E. Impact of the cold shock phenomenon on quantification of intracellular metabolites in bacteria. *Anal Biochem.* 2004;327:135–139.
64. Zakhartsev M, Winterhauer O, Horn T, Yang XL, Reuss M. Fast sampling for quantitative microbial metabolomics: New aspects on cold methanol quenching: Metabolite coprecipitation. *Metabolomics.* 2015;11:286–301.
65. Noack S, Wiechert W. Quantitative metabolomics: A phantom? *Trends Biotechnol.* 2014;32:238–244.
66. Douma RD, de Jonge LP, Jonker CT, Seifar RM, Heijnen JJ, van Gulik WM. Intracellular metabolite determination in the presence of extracellular abundance: Application to the penicillin biosynthesis pathway in *Penicillium chrysogenum*. *Biotechnol Bioeng.* 2010;107:105–115.
67. Canelas AB, ten Pierick A, Ras C, et al. Quantitative evaluation of intracellular metabolite extraction techniques for yeast metabolomics. *Anal Chem* 2009;81:7379–7389.
68. Dietmair S, Timmins NE, Gray PP, Nielsen LK, Kromer JO. Towards quantitative metabolomics of mammalian cells: Development of a metabolite extraction protocol. *Anal Biochem.* 2010;404:155–164.
69. Maharjan RP, Ferenci T. Global metabolite analysis: The influence of extraction methodology on metabolome profiles of *Escherichia coli*. *Anal Biochem.* 2003;313:145–154.
70. Winder CL, Dunn WB, Schuler S, et al. Global metabolic profiling of *Escherichia coli* cultures: An evaluation of methods for quenching and extraction of intracellular metabolites. *Anal Chem.* 2008;80:2939–2948.
71. Hajjaj H, Blanc P, Goma G, Francois J. Sampling techniques and comparative extraction procedures for quantitative determination of intra- and extracellular metabolites in filamentous fungi. *Fems Microbiol Lett.* 1998;164:195–200.
72. Gonzalez B, François J, Renaud M. A rapid and reliable method for metabolite extraction in yeast using boiling buffered ethanol. *Yeast.* 1997;13:1347–1355.
73. Sellick CA, Knight D, Croxford AS, et al. Evaluation of extraction processes for intracellular metabolite profiling of mammalian cells: Matching extraction approaches to cell type and metabolite targets. *Metabolomics.* 2010;6:427–438.
74. Wu L, Mashego MR, van Dam JC, et al. Quantitative analysis of the microbial metabolome by isotope dilution mass spectrometry using uniformly ¹³C-labeled cell extracts as internal standards. *Anal Biochem.* 2005;336:164–171.
75. Mashego MR, Wu L, Van Dam JC, et al. MIRACLE: Mass isotopomer ratio analysis of U-¹³C-labeled extracts. A new method for accurate quantification of changes in concentrations of intracellular metabolites. *Biotechnol Bioeng.* 2004;85:620–628.
76. Bennett BD, Yuan J, Kimball EH, Rabinowitz JD. Absolute quantitation of intracellular metabolite concentrations by an isotope ratio-based approach. *Nat Protoc.* 2008;3:1299–311.
77. Patacq C, Chaudet N, Letisse F. Absolute quantification of ppGpp and pppGpp by double-spike isotope dilution ion chromatography-high-resolution mass spectrometry. *Anal Chem.* 2018;90:10715–10723.
78. Schatschneider S, Abdelrazig S, Safo L, et al. Quantitative isotope-dilution high-resolution-mass-spectrometry analysis of multiple intracellular metabolites in *Clostridium autoethanogenum* with uniformly (¹³C)-labeled standards derived from spirulina. *Anal Chem.* 2018;90:4470–4477.
79. Seifar RM, Zhao Z, van Dam J, van Winden W, van Gulik W, Heijnen JJ. Quantitative analysis of metabolites in complex biological samples using ion-pair reversed-phase liquid chromatography-isotope dilution tandem mass spectrometry. *J Chromatogr A.* 2008;1187:103–110.
80. Stafnes MH, Rost LM, Bruheim P. Improved phosphometabolome profiling applying isotope dilution strategy and capillary ion chromatography-tandem mass spectrometry. *J Chromatogr B.* 2018;1083:278–283.
81. Vielhauer O, Zakhartsev M, Horn T, Takors R, Reuss M. Simplified absolute metabolite quantification by gas chromatography-isotope dilution mass spectrometry on the basis of commercially available source material. *J Chromatogr B.* 2011;879:3859–3870.
82. Wang G, Wu B, Zhao J, et al. Power input effects on degeneration in prolonged penicillin chemostat cultures: A systems analysis at flux, residual glucose, metabolite, and transcript levels. *Biotechnol Bioeng.* 2018;115:114–125.

83. van Gulik WM, de Laat WT, Vinke JL, Heijnen JJ. Application of metabolic flux analysis for the identification of metabolic bottlenecks in the biosynthesis of penicillin-G. *Biotechnol Bioeng*. 2000;68:602–618.
84. Lee JW, Na D, Park JM, Lee J, Choi S, Lee SY. Systems metabolic engineering of microorganisms for natural and non-natural chemicals. *Nat Chem Biol*. 2012;8:536–546.
85. Ellis DI, Goodacre R. Metabolomics-assisted synthetic biology. *Curr Opin Biotechnol*. 2012;23:22–28.
86. Hasunuma T, Sanda T, Yamada R, Yoshimura K, Ishii J, Kondo A. Metabolic pathway engineering based on metabolomics confers acetic and formic acid tolerance to a recombinant xylose-fermenting strain of *Saccharomyces cerevisiae*. *Microb Cell Fact*. 2011;10:2.
87. de Jonge Lp, Buijs NA, Heijnen JJ, van Gulik WM, Abate A, Wahl SA. Flux response of glycolysis and storage metabolism during rapid feast/famine conditions in *Penicillium chrysogenum* using dynamic (13) C labeling. *Biotechnol J*. 2014;9:372–385.
88. Zhao Z, Ten Pierick A, de Jonge L, Heijnen JJ, Wahl SA. Substrate cycles in *Penicillium chrysogenum* quantified by isotopic non-stationary flux analysis. *Microb Cell Fact*. 2012;11:140.
89. Wang X, Zhao J, Xia J, Wang G, Chu J, Zhuang Y. Impact of altered trehalose metabolism on physiological response of *Penicillium chrysogenum* chemostat cultures during industrially relevant rapid feast/famine conditions. *Processes*. 2021;9:118–134.
90. Vavricka CJ, Hasunuma T, Kondo A. Dynamic metabolomics for engineering biology: Accelerating learning cycles for bioproduction. *Trends Biotechnol*. 2020;38:68–82.
91. Buescher JM, Liebermeister W, Jules M, et al. Global network reorganization during dynamic adaptations of *Bacillus subtilis* metabolism. *Science*. 2012;335:1099–1103.
92. Wiechert W, Noack S. Mechanistic pathway modeling for industrial biotechnology: Challenging but worthwhile. *Curr Opin Biotechnol*. 2011;22:604–610.
93. Gombert AK, Nielsen J. Mathematical modelling of metabolism. *Curr Opin Biotech*. 2000;11:180–186.
94. Dano S, Madsen MF, Schmidt H, Cedersund G. Reduction of a biochemical model with preservation of its basic dynamic properties. *Febs J*. 2006;273:4862–4877.
95. de Jonge LP, Buijs NA, ten Pierick A, et al. Scale-down of penicillin production in *Penicillium chrysogenum*. *Biotechnol J*. 2011;6:944–958.
96. Haringa C, Mudde RF, Noorman HJ. From industrial fermentor to CFD-guided downscaling: What have we learned? *Biochem Eng J*. 2018;140:57–71.
97. Lapin A, Klann M, Reuss M. Multi-scale spatio-temporal modeling: Lifelines of microorganisms in bioreactors and tracking molecules in cells. *Adv Biochem Eng Biotechnol*. 2010;121:23–43.
98. Lapin A, Muller D, Reuss M. Dynamic behavior of microbial populations in stirred bioreactors simulated with Euler-Lagrange methods: Traveling along the lifelines of single cells. *Ind Eng Chem Res*. 2004;43:4647–4656.
99. Lapin A, Schmid J, Reuss M. Modeling the dynamics of *E. coli* populations in the three-dimensional turbulent field of a stirred-tank bioreactor—A structured–segregated approach. *Chem Eng Sci*. 2006;61:4783–4797.
100. Haringa C, Tang WJ, Wang G, et al. Computational fluid dynamics simulation of an industrial *P. chrysogenum* fermentation with a coupled 9-pool metabolic model: Towards rational scale-down and design optimization. *Chem Eng Sci*. 2018;175:12–24.
101. Humphrey A. Shake flask to fermentor: What have we learned? *Biotechnol Progr*. 1998;14:3–7.
102. Wang G, Tang WJ, Xia JY, Chu J, Noorman H, van Gulik WM. Integration of microbial kinetics and fluid dynamics toward model-driven scale-up of industrial bioprocesses. *Eng Life Sci*. 2015;15:20–29.